RBME-00140-2023

Advances in Microsphere-based Super-resolution Imaging

Neil Upreti,[1] Geonsoo Jin,[2] Joseph Rich,[1] Ruoyu Zhong,[2] John Mai,[3] Chenglong Zhao,[4] and Tony Jun Huang[1,2]**

[1] Department of Biomedical Engineering, Duke University, Durham, NC 27708, USA

[2] Thomas Lord Department of Mechanical Engineering and Material Science, Duke University, Durham, NC 27708, USA

[3] Alfred E. Mann Institute, University of Southern California, Los Angeles, CA 90089, USA

[4] The MITRE Corporation, McLean, VA 22102, USA

*To whom correspondence should be addressed. Email: czhao@mitre.org; tony.huang@duke.edu

***Abstract*—Techniques to resolve images beyond the diffraction limit of light with a large field of view (FOV) are necessary to foster progress in various fields such as cell and molecular biology, biophysics, and nanotechnology, where nanoscale resolution is crucial for understanding the intricate details of large-scale molecular interactions. Although several means of achieving super-resolutions exist, they are often hindered by factors such as high costs, significant complexity, lengthy processing times, and the classical tradeoff between image resolution and FOV. Microsphere-based super-resolution imaging has emerged as a promising approach to address these limitations. In this review, we delve into the theoretical underpinnings of microsphere-based imaging and the associated photonic nanojet. This is followed by a comprehensive exploration of various microsphere-based imaging techniques, encompassing static imaging, mechanical scanning, optical scanning, and acoustofluidic scanning methodologies. This review concludes with a forward-looking perspective on the potential applications and future scientific directions of this innovative technology.**

***Index Terms*—Photonic nanojets, Microsphere, Scanning nanoscope, Super-resolution imaging, Enlarged field of view**

I. INTRODUCTION

Microscopy has been instrumental in driving significant advancements in science, engineering, and medicine.[1-3] The initial development of basic optical microscopes by pioneers such as Robert Hooke and Anton Van Leeuwenhoek paved the way for observing cells and bacteria, leading to pivotal discoveries in the realm of biology.[4,5] Today, microscopes are utilized in diverse contexts, ranging from electron microscopes for providing structural insights of proteins and viruses to scanning probe microscopes for characterizing colloidal particles, assembling nanostructures, and creating dopant profiles for semiconductors.[6-15]

The most common type of microscopy, optical microscopy, always faces two interrelated bottlenecks and tradeoffs: overcoming light's diffraction limit and balancing FOV with image resolution. Usually, the resolution of an optical imaging system is constrained by the diffraction limit, *i.e.*, the smallest spacing between structures that the system can resolve. Typically, the resolution is inversely related to the numerical aperture (NA) of the objective lens utilized. A higher NA leads to enhanced resolution, yet it results in a reduced FOV.[16] Because of physical constraints, commercial objective lenses have a maximum NA of around 1.49.[17] Although a higher NA can be achieved using a solid immersion lens, its intrusive nature and the need for direct contact with the subject being imaged make it less practical for many situations.[18-23] A widely used approach to attain high resolution alongside an extensive FOV is by mechanically scanning the sample under a high-NA objective lens and merging these captured images to digitally expand the FOV in a resulting composite image. However, this method can be time-consuming due to the need for multiple image captures and digital processing, and the resolution is still limited by diffraction.

In the quest for super-resolution, optical microscopy stands as the foundational technique, yet its capabilities are inherently limited by the diffraction limit of light. To transcend this barrier, various advanced methodologies have been developed. Wide-field microscopy scales up the imaging process to encompass entire fields simultaneously, but it still grapples with the constraints of diffraction.[24-28] Near-field microscopy breaks through these constraints using a tapered optical fiber tip to collect evanescent waves, allowing for finer resolutions.[29-33] Innovative optical design-based techniques such as metalenses, with their capacity for nanoscale light focusing, and silver superlenses that harness plasmonic effects offer substantial resolution enhancements.[34-47] Fluorescence-based techniques have also seen remarkable progress: Stimulated Emission Depletion (STED) Microscopy employs stimulated emission to narrow down the emission volume, thus achieving higher resolution; Photo-Activated Localization Microscopy (PALM) and Stochastic Optical Reconstruction Microscopy (STORM) utilize photo-activated and stochastic imaging principles respectively to achieve molecular-scale imaging; while Structured Illumination Microscopy (SIM) leverages structured illumination to improve spatial resolution beyond the conventional limits.[48-64] While the various existing methods bring us closer to the ideal of high image resolution and an expansive FOV, they come with their own set of challenges, such as complexity of setup, slower imaging speeds, and FOV limitations; thus, they can typically only address one of the shortcomings (*e.g.*, resolution, processing time, or FOV) but not all.[65-82] Therefore, there is considerable interest in

enhancing the imaging capabilities of conventional optical microscopes and improving these platforms with the following desirable features: super-resolution imaging beyond the diffraction limit with a large FOV, easy-to-implement imaging processing algorithms, and compatibility with existing commercial microscopes without significant modifications.

Microsphere-based imaging technology has emerged as a means for realizing these desired features. It offers super-resolution imaging with a large FOV through its lens-like ability to focus light at a higher resolution than conventional microscope optics. Additionally, using multiple microspheres ensures that imaging is not restricted to a single point. By combining microsphere manipulation technologies and image processing algorithms, individual images can be seamlessly and efficiently merged to produce large, high-resolution images. Coupling microsphere-based imaging with conventional microscopy enables many diverse applications for researchers in a variety of scientific and clinical fields.

Thus, microsphere-based microscopy offers an alternative approach, leveraging dielectric microspheres to capture and magnify evanescent waves. Unlike the aforementioned methods, it can be simpler in setup, especially in static imaging scenarios, and offers versatility in the types of samples it can image. Although microsphere-based microscopy surmounts many of the challenges seen in existing technology, it still has significant room for optimization. However, its compatibility with conventional microscopy setups and potential for broader applications make it a promising avenue for super-resolution imaging. Further comparisons between existing super-resolution techniques and microspheres can be seen in Table 1.

This article summarizes recent developments in microsphere-based super-resolution microscopy and elaborates on how this technology solves the aforementioned problems, enabling high-resolution, large FOV imaging of biologically relevant samples such as cells and viruses with a large FOV. The review is organized as follows: the mechanism enabling microsphere-based super-resolution imaging and the associated photonic nanojet effect, super-resolution imaging by applying static microspheres, and super-resolution imaging by scanning microspheres to increase the FOV. This review concludes by exploring potential uses for the technology and future possibilities in the realm of 3D microsphere-based imaging.

Table 1. Existing Techniques Compared with Microsphere-Based Microscopy

Technique	Conventional Optical Microscopy [1]	Near-Field Microscopy [29-33]	Metalenses [34-39]	Superlenses [40-47]	STED Microscopy [48-50]	PALM [51-54] / STORM [55-59]	SIM [60-64]	Microsphere-Based Microscopy [104-129]
Principle	Far-field light collection	Near-field light collection	Far-field light collection	Near-field light collection	Far-field fluorescence light & depletion	Far-field fluorescence from single-molecule & localization	Structured far-field light	Near-field light
Resolution	~200 nm (diffraction limit of light)	~20 - 50 nm	~200 nm	~50 nm - 100 nm	~20 - 30 nm	~ 20 - 60 nm	~100 - 130 nm	~20 nm
Cellular Imaging	**Live/Dead**	**Dead**	**Live/Dead**	**Dead**	**Dead**	**Live/Dead**	**Live/Dead**	**Live/Dead**
Imaging Modes (Transmission, Reflection, Fluorescent, or Multiple)	**Multiple**	**N/A**	**Multiple**	**Multiple**	**Fluorescent**	**Fluorescent**	**Multiple**	**Multiple**
Setup Complexity	**Low**	**Very high**	**Moderate**	**High**	**High**	**High**	**Moderate**	**Low**
Risk of Sample Damage	**Low**	**High**	**Low**	**Moderate**	**High**	**High**	**Low**	**Low**
Advantages	Broadly accessible, diverse contrast methods	Nanoscale resolution	Small form factor and compact design	Nanoscale resolution	Real-time imaging, compatible with standard labels	Molecular-scale imaging, versatile probe compatibility	Quicker than PALM/STORM, low phototoxicity	High resolution and large field-of-view simultaneously, easy integration with microscopes
Disadvantages	diffraction limit, trade-off between resolution and field of view	small sample-tip distance, long imaging time, complex setup	High-manufacturing cost, complex design process, technology not matured	Direct sample-lens contact with limited use cases, complex fabrication, large signal losses	High photobleaching risk, complex setup with multiple laser sources	Slow imaging speed and complex optical setup, require additional steps for image recovery	Limited resolution improvement and requires additional steps for image recovery	Requires additional steps for microsphere scanning and image recovery

This article has been accepted for publication in IEEE Reviews in Biomedical Engineering. This is the author's version which has not been fully edited and content may change prior to final publication. Citation information: DOI 10.1109/RBME.2024.3355875

II. Mechanism for Microsphere-based Super-Resolution Imaging

The capability for super-resolution imaging using microspheres is facilitated by the phenomenon known as the photonic nanojet effect. When a plane electromagnetic wave illuminates a transparent microsphere, this phenomenon occurs.[89-96] The plane electromagnetic wave is focused into a narrow, high-intensity beam near the microsphere that propagates and extends several wavelengths along its optical path. Crucially, the photonic nanojet, which is the beam focused by the microsphere, has a width smaller than the classical diffraction limit. This characteristic enables the enhancement of resolution in standard optical microscopes.

The origin of the photonic nanojet effect is a complex scattering and interference process that has been investigated previously.[97-101] As light interacts with the microsphere, it undergoes both constructive and destructive interference.[102] The constructive interference results in a highly concentrated, sub-wavelength light beam beyond the microsphere. The photonic nanojet from a transparent microsphere can be fully described by applying Mie scattering theory, which allows for the full exploitation and optimization of this focusing property.

A typical imaging setup using a microsphere-based photonic nanojet is depicted in Fig. 1a. A microsphere is positioned above the sample, and the sample is first imaged with this microsphere. Then this image passes through the imaging system of a commercial microscope without any further modification of the optical path. Fig. 1b shows a numerical simulation of the wavefront interactions demonstrating the focusing capability of a $BaTiO_3$ microsphere. Light is focused to a focal point with a full width at half maximum (FWHM) of 135 nm. This is below the optical diffraction limit, typically half of the wavelength, as shown in Fig. 1c. The photonic nanojet can also extend over ~2λ past the microsphere with an intensity ~1000x greater than the wavelength of the incoming beam.[103]

In the context of microsphere-based super-resolution imaging, several parameters are used to optimize the imaging property (Fig. 1d), *e.g.*, the difference in refractive index between the microsphere and its surrounding medium, the diameter of the microsphere, along with the wavelength, polarization, and phase of the light used for illumination. Changing these parameters typically does not require a significant alteration in the configuration of the optical microscope. For example, changing the radius of the microsphere can be easily achieved by changing the types of microspheres on the imaging sample. The wavelength and polarization of the illumination light can be readily changed by rotating the built-in filter sets or inserting a polarizer within a commercial microscope, respectively. Therefore, it provides an effective yet simple way to integrate this technology directly into a commercial optical microscope.

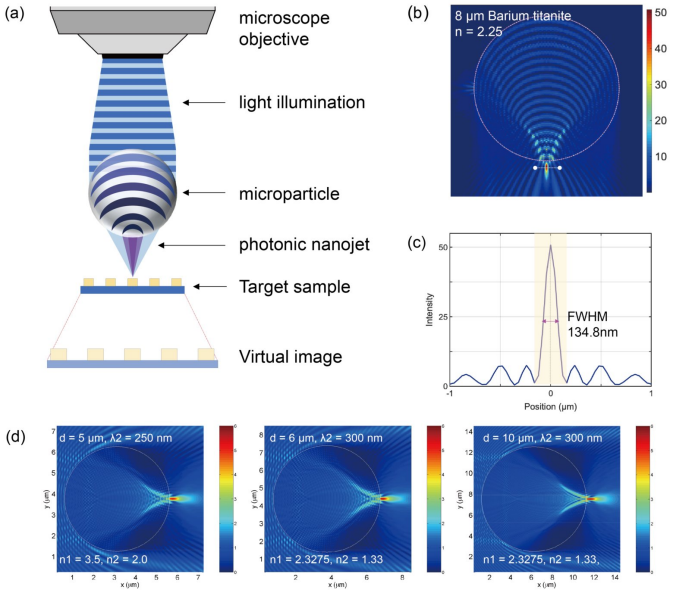

Fig. 1. Mechanism of microsphere-based super-resolution imaging. (a) Diagram illustrating the concept of super-resolution imaging using microspheres. (b) A numerical simulation mapping the interactions of the optical wavefronts, which produce the effects of super-resolution from a microparticle. (c) A line profile across the focal point obtained from numerical simulation reveals a full-width at half-maximum (FWHM) measurement of 134.8 nm. This is calculated for a barium titanate microparticle with a diameter of 8 μm and a refractive index of 2.25. (d) Simulation results for three different combinations of parameters and the resulting photonic nanojets. In this context, λ2 refers to the wavelength of light, n1 is the dielectric cylinder's refractive index, D denotes the cylinder's diameter, and n2 indicates the external medium's refractive index.[103] Copyright 2009, Journal of Computational and Theoretical Nanoscience.

III. Super-Resolution Imaging Based on Static Microspheres

Early approaches to microsphere-based super-resolution imaging relied on the use of microspheres that were stationary throughout the imaging process. Nonetheless, these methods enabled direct super-resolution imaging, allowing for image capture directly from the microsphere without requiring additional post-processing steps. As a result, static microsphere-based imaging techniques are both efficient and straightforward to implement but with a limited FOV.

A. Super-Resolution Imaging with a Freestanding Microsphere

A remarkable resolution of ~50 nm was achieved by Wang *et al.* with stationary SiO_2 microspheres and a bright-field microscope equipped with an 80× objective lens (NA = 0.9, Olympus MDPlan).[104] The imaging captured through single SiO_2 microspheres (n = 1.46) with diameters ranging from 2 μm to 9 μm was studied. Illumination was provided by a white light halogen lamp, and experiments were carried out in both transmission and reflection modes. In transmission mode, the sample transmits light that is used by the microspheres to form a virtual image of the sample. This virtual image is then

projected into a conventional optical microscope to render the final image. The transmission mode is ideal for imaging transparent or semi-transparent samples. In reflection mode, the incident light is first focused by the microsphere and then reflected off the sample and a virtual image is formed after the reflected light has returned along the same optical path through the single microsphere. The reflection mode is appropriate for imaging of non-transparent samples.

Two nanostructures were used to test the imaging capabilities of the SiO_2 microspheres in transmission mode, displayed in the left section of Fig. 2b. One was a grating with a line space of 360 nm fabricated on a glass substrate. The other nanostructure was a thin gold film with 50 nm diameter holes on the surface. The right panel of Fig. 2b shows corresponding images of the two different test nanostructures obtained with and without the microspheres, respectively. The nanostructures beneath the microspheres are clearly resolved. In contrast, they cannot be resolved directly using the optical microscope without microspheres. A significant improvement in the resolution is also obvious in the reflection mode, as shown in Fig. 2c. Imaging of a nanograting and a nanostar was used as the test target in the reflection mode. However, this method has two shortcomings: (1) repositioning of the microsphere is required for imaging of large sample areas and is especially time-consuming; (2) precisely positioning the microsphere above the sample for ideal imaging results can be challenging.

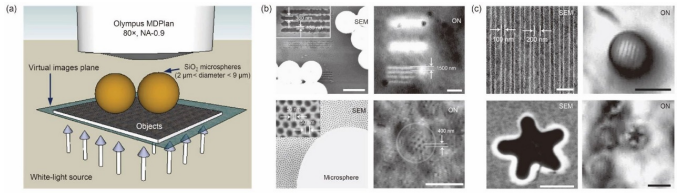

Fig. 2. Imaging nanostructures by a white-light microsphere nanoscope. (a) Schematic of microsphere imaging in transmission mode. Target objects and SiO2 microspheres, ranging in diameter from 2 μm to 9 μm, are illuminated by a white-light source. The light then travels into a standard microscope, enabling the visualization of the near-field objective target. (b) SEM images of the 360 nm grating lines, featuring a 130 nm pitch and 50 nm pores, are presented in the left panels (scale bar: 5 μm). In the right panels, images captured through microspheres in transmission mode display the targets. The magnification factor between panels was calculated to be approximately 8. A microsphere with a diameter of 2.37 μm was utilized to achieve this result. (c) Imaging with microspheres (2.37 μm) in reflection mode is depicted. In the left panels, SEM images reveal 200 nm grating lines with a 100 nm pitch alongside a star-shaped structure. On the right, images captured via microspheres display these targets (scale bars: Left (500 nm), Right (5 μm)).[104] Copyright 2011, Nature Communications.

Later, a liquid medium, rather than air, was utilized due to the potential enhancement in microsphere imaging performance because of the difference in refraction indices. Li *et al.* was able to image 75 nm adenoviruses using transparent submerged microsphere optical nanoscopy (SMON) with $BaTiO_3$ microspheres in deionized water.[105] $BaTiO_3$ microspheres, each measuring 100 μm in diameter, were positioned on the specimen, and deionized water was utilized to fill the gap between the specimen and the objective lens so that the microspheres were completely submerged in water, as shown in Fig. 3a. The left and right panels of Fig. 3b show the SEM image and SMON image of virus clusters using $BaTiO_3$ microspheres, respectively. However, the small gap required between the specimen and the objective lens is not convenient for use in practical applications.

The SMON technique, which eliminates the need for fluorescent tagging, has been demonstrated to be compatible with samples ranging from biological specimens to nanoscale materials and is easily integrated with existing microscopes. However, it also has a few limitations: (1) The technique depends entirely on a microsphere-substrate interface where the microsphere directly interacts with the specimen. This may not be suitable for many samples or imaging conditions. (2) The technology is far more suited for surface imaging rather than 3D imaging. (3) The space separating the microsphere and the objective lens is extremely limited, making it possible for issues to arise when precise control affects imaging consistency.

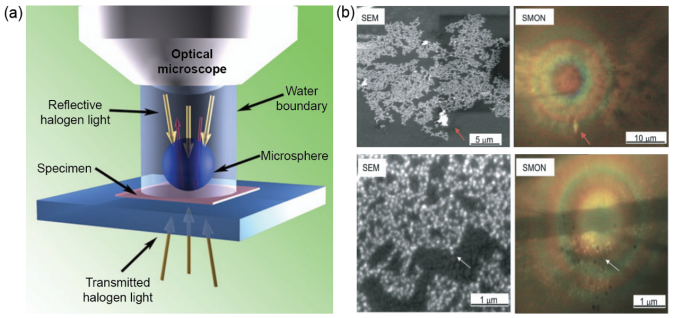

Fig. 3. Submerged Microsphere Optical Nanoscopy (SMON) imaging. (a) A diagram illustrating nano-imaging using the SMON technique, featuring a BaTiO3 microsphere submerged in water. (b) Virus cluster images taken by SEM (left). The same cluster imaged by SMON and magnified with an objective lens.[105] Copyright 2013, Light: Science & Applications.

Moving away from SMON, we now focus on the work by Yang *et al.,*[106] investigating the effect of different mediums on the microsphere imaging resolution. In this research, glass microspheres (n = 1.92) were employed, as shown in Fig. 4a. Instead of using bright-field imaging as discussed in the previous two examples, fluorescent imaging through a glass microsphere is performed without modifications to the original optical path of the optical microscope. The fluorescent signal from stained centrioles, mitochondria, and chromosomes was collected by the glass microspheres, and the structures were successfully resolved, as shown in Fig. 4b-d. Furthermore, the utilization of microspheres enabled the observation of changes in mitochondrial-encoded protein expression due to doxycycline treatment in a mouse liver cell line. This result was achieved by staining antibodies and placing the microsphere upon the liver organelle being observed.

This article has been accepted for publication in IEEE Reviews in Biomedical Engineering. This is the author's version which has not been fully edited and content may change prior to final publication. Citation information: DOI 10.1109/RBME.2024.3355875

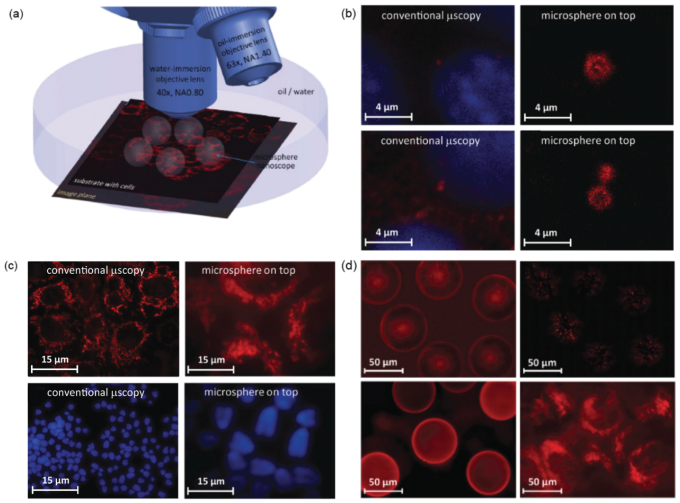

Fig. 4. Microsphere nanoscope. (a) Schematic for a microsphere nanoscope: Glass microspheres on cell surfaces project near-field optical information as magnified virtual images, resolvable by a standard microscope objective. (b) Comparing traditional fluorescence microscopy (left) and a microsphere nanoscope (right) for imaging of fluorescent AML12 cell structures, the nanoscope clearly resolves γ-tubulin on centrioles with a dot-in-ring pattern, using anti-γ-tubulin Ab, Dylight® 649-conjugated secondary Ab, and Hoechst 33342 for nucleus staining (in blue). (c) Mitochondria images using MitoTracker® probe. Chromosome images stained with DAPI. (d) Multiple microsphere nanoscopes are in the FOV of a 40x water immersion objective. It is important to note the figures in the left and right columns were taken at different depths. Fluorescent images (top row) display 100 nm nanoparticles on a glass substrate and AML12 cells with mitochondrial stain. Fluorescent images (bottom row) simultaneously detect multiple areas with 100 nm nanoparticles and mitochondria.[106] Copyright 2014, Small.

While the successful imaging of samples in a liquid environment is encouraging for a wide range of applications, especially for biological studies, the best imaging conditions and parameters for a given microsphere in a liquid environment need to be evaluated to guide practical applications. Yang *et al.* performed such a study by employing $BaTiO_3$ microspheres to image nanostructures immersed in water, as shown in Fig. 5a.[107] Both simulations and experiments were performed to evaluate the relationship between the size of the microspheres and the beam waist size of the resulting photonic nanojets, which is directly related to the imaging resolution. The beam waists of photonic nanojets from $BaTiO_3$ microspheres, which ranged from 2 μm to 20 μm, were studied.

The results show that the photonic nanojet with the smallest beam waist and best-resulting resolution is obtained from a microsphere measuring 6 μm in diameter. The top panel in Fig. 5b shows the focusing capability, defined as the ratio (L/l) of the width of the incident beam before entering the microsphere (L) to that of the photonic nanojet after the microsphere (l), based on the size of the microsphere's diameter. A peak in the focusing capability is shown for a 6 μm microsphere, representing the most focusing power. Note that the size effect of the microsphere is already considered in this parameter, *i.e.*, the width of the incident beam decreases with a decrease in microsphere size. The lower panel in Fig. 5b shows the beam waist of the photonic nanojet in terms of the illumination wavelength (w/λ) as a function of the microsphere size, which shows a minimum (w=0.38 λ) for a microsphere with a diameter of 6 μm.

A nanograting structure with a line spacing of 100 nm was used for testing, as shown in the top panel of Fig. 5c. A standard optical microscope equipped with a water-immersion objective (NA = 0.8) is unable to resolve the nanograting. without microspheres, as shown in the lower panel of Fig. 5c. However, the details of the nanograting are well resolved by adding microspheres with a diameter of 4.1 and 7.1 μm, respectively, as shown in Fig. 5d. But the larger microsphere (7.1 μm) results in better image quality than that from the smaller one.

In essence, using standalone microspheres for optical imaging offers a straightforward method to enhance the resolution of current optical microscopes without major modifications to the optical setup. These imaging improvements can be easily tailored to the desired target by changing the various parameters mentioned above. However, this method also leads to the following limitations in practical application: (1) the imaging region of interest cannot be changed due to the static nature of the microsphere on the sample surface; (2) the increase in the resolution by applying a microsphere is achieved by significantly reducing the FOV. For example, the FOV cannot exceed the microsphere's size. In fact, it is typically smaller than the size of the microsphere, and only the center part of the image can be used due to significant aberrations caused at the edge of the microsphere. Despite these limitations, optical imaging with standalone microspheres is ideal for novices wanting to perform initial experiments with any conventional microscope while minimizing the learning curve typically experienced with other state-of-the-art optical techniques.

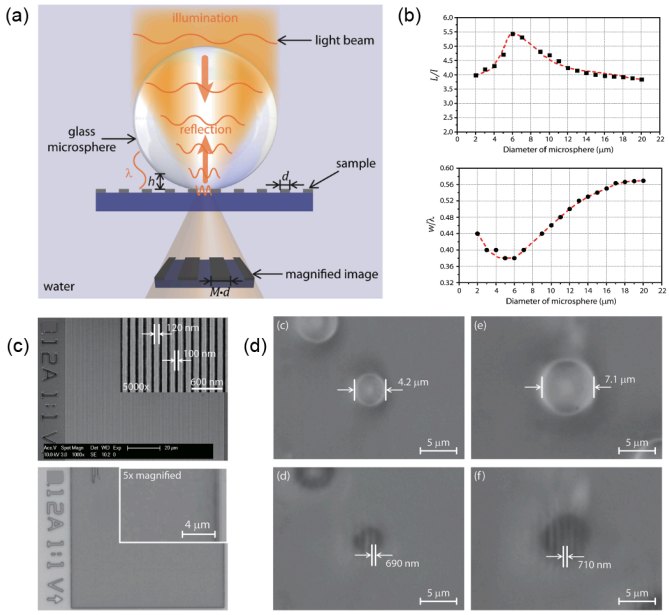

Fig. 5. Imaging with static microspheres and the variation in magnification factors corresponding to microspheres of

This article has been accepted for publication in IEEE Reviews in Biomedical Engineering. This is the author's version which has not been fully edited and content may change prior to final publication. Citation information: DOI 10.1109/RBME.2024.3355875

various sizes. (a) A diagram representing the process of imaging with microspheres and the associated magnification factor, M. (b) Results from Finite Element Method (FEM) simulations demonstrating the light-focusing abilities of microspheres with varying diameters. The ratio L/l represents the comparison between the incident light's width entering the microsphere and the focused light's width exiting it. Additionally, FEM simulation outcomes are normalized to the ratio of the width of photonic nanojets to the wavelength of the illuminated light, denoted as w/λ, for microspheres of different diameters. (c) The top panel displays an SEM image of the nanostructured grating target, which includes lines that are 120 nm wide with a 100 nm pitch. The bottom panel shows the image captured using a 40x water-immersion objective (NA = 0.8). (d) Images of the grating nanostructure obtained through microsphere imaging, employing microspheres of sizes 4.2 and 7.1 μm, are presented respectively.[107] Copyright 2016, Nano Letters.

B. Imaging with the Microsphere Embedded in a Matrix

The drop-casting technique, which entails depositing a droplet laden with microspheres onto a substrate and allowing it to dry, has been found to have significant limitations for super-resolution imaging applications. The inherent randomness of this method results in inconsistencies and imprecision in microsphere placement on sample surfaces, thereby hindering imaging performance. Consequently, researchers pursued more controlled approaches to apply microspheres, aiming to enhance the reproducibility and accuracy of the imaging process.

Darafsheh *et al.* explored one such strategy by embedding microspheres within transparent, solidified films (elastomers) to provide improved control over position and orientation.[108] By securing the microspheres in a well-defined structure, researchers could circumvent the shortcomings of drop-casting and optimize microsphere-based imaging systems for more precise, higher-resolution imaging outcomes. By using this technique, they were able to exceed the diffraction limit and attain a resolution under 200 nm. The absence of fluid in this technique was advantageous as it prevented damage to certain biological samples. Furthermore, microsphere-embedded elastomers could be prepared beforehand and utilized as coverslips, conserving the time and effort previously spent on individual microsphere placement. The experimental setup shown in Fig. 6(a-b) resembles SMON. In this configuration, the elastomer is positioned above the specimen, and images are captured using an upright microscope in reflection illumination mode. This microscope is utilized to magnify the virtual images. Fig. 6(c-d) shows a Blu-ray disc imaged using this technique. The technique also showed success when imaging biological samples. In Fig. 6(e-f), a microsphere was used to significantly enhance the imaging of glioblastoma cells. Additionally, Fig. 6(g-h) shows a similar enhancement when using microspheres to image the nuclei of a cell and double-stranded DNA breaks present within.

Nonetheless, this technology has several drawbacks: (1) Embedding microspheres in a matrix can be more intricate and time-consuming than conventional drop-casting methods. (2) The matrix material may negatively impact the imaging capabilities of the microspheres and restrict their performance in specific applications. (3) The rigidity of the matrix could potentially reduce the imaging system's flexibility and adaptability for textured samples, obstructing the acquisition of images in certain areas. (4) Lastly, as the matrix immobilizes the microspheres, it may not be suitable for dynamic imaging scenarios requiring rapid adjustments to microsphere positions.

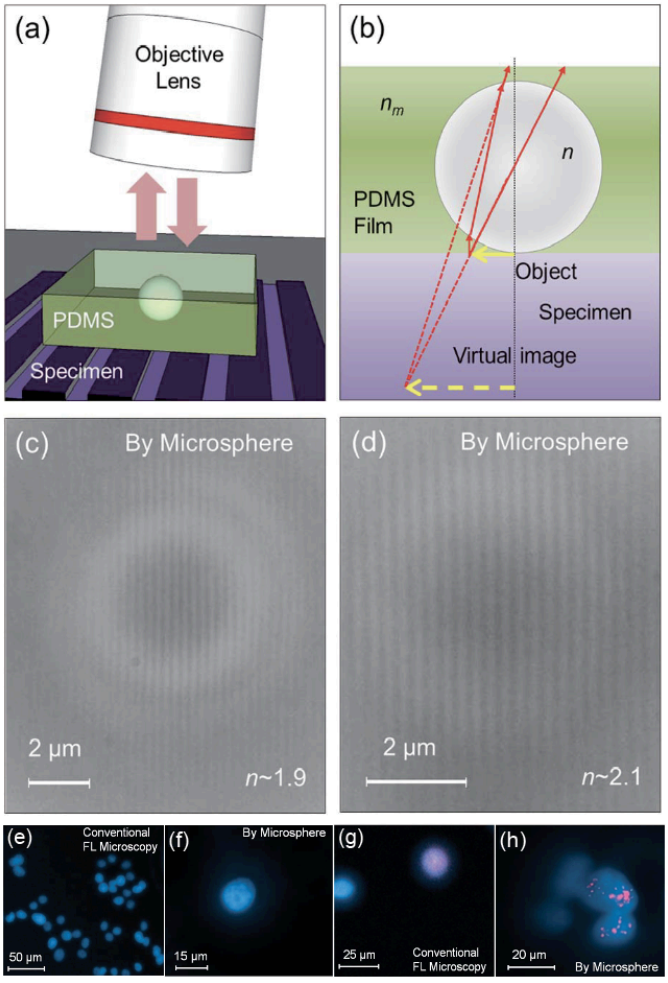

Fig. 6. Imaging using an elastomer-embedded microsphere. (a) A specimen was prepared by embedding a microsphere in a PDMS film and positioning it on the target. (b) A side view illustrates the interface between the microsphere and the specimen, which is instrumental in generating the virtual image. (c-d) Structures with a width of 200 nm and a pitch of 100 nm were captured using BaTiO3 microspheres: (c) a 65 μm microsphere and (d) a 55 μm microsphere (displayed in the bottom right). (e-f) fluorescent visualization of U87 glioblastoma cells (e) without the presence of a microsphere and (f) with a $BaTiO_3$ sphere of 130 μm diameter embedded in PDMS and DAPI. (g-h) Imaging cell nuclei and radiation-induced foci (g) in the absence of, and (h) with the incorporation of a microsphere. (h) Double-stranded DNA breaks, which appear as red foci, are discernible through the sphere.[108] Copyright 2015, Optics Letters.

C. Static Microsphere-based Imaging with Other Types of Microscopy

Capitalizing on the achievements of static microsphere imaging, researchers continued to investigate a wide array of possibilities to fully harness the technology's latent potential. This involved experimenting with various liquid media and imaging methods beyond traditional microscopy, with the objective of determining the optimal configuration through comprehensive and systematic experimentation.

For instance, through the application of coherent anti-Stokes Raman scattering (CARS) microscopy, scientists were able to capture images of sub-diffraction elements on a Blu-ray disc using SiO2 microspheres. They achieved an impressive lateral magnification of 5.0×, leading to a minimum lateral resolution of 200 nm. The study also revealed that the resolution was significantly influenced by variations in the size of the microsphere, the position of the laser beam's focal plane, and the refractive index. Through the application of CARS microscopy, scientists were able to capture images of sub-diffraction elements on a Blu-ray disc using SiO2 microspheres. They achieved an impressive lateral magnification of 5.0×, leading to a minimum lateral resolution of 200 nm. The study also revealed that the resolution was significantly influenced by variations in the size of the microsphere, the position of the laser beam's focal plane, and the refractive index.

A reduction in microsphere size led to a corresponding decrease in the beam waist of the focal point, allowing for the imaging of exceptionally small features. Adjusting the position of the laser beam focal plane influenced the resolution, as it altered the distance between axial lens points and subsequently affected image clarity. Finally, the focusing on the subject was influenced by the microsphere's refractive index, with higher refractive indices generally improving focus and resolution.

Yan *et al.* modified the traditional setup, achieving an impressive lateral resolution of 25 nm was achieved by directing a laser through microspheres made of fused silica and polystyrene at an angle.[109] The image underwent further processing through a scanning laser confocal microscope (SLCM). Utilizing a single 408 nm laser beam, which was steered by galvanometric mirrors, the laser penetrated the microspheres. This process resulted in the creation of a central light lobe that was focused and smaller than the laser's wavelength. This focused light interacted with the sample, producing a reflection pattern called a subwavelength reflecting cross-section. In essence, the focused light resolved minuscule details on the sample's surface, smaller than the wavelength of the laser. The SLCM captured the reflected light, and the pinhole filtering effect enhanced the signal-to-noise ratio by reducing external noise, yielding a crisper, higher-resolution image. As a result, intensity-based point-scan imaging allowed for a 25 nm lateral resolution. This innovative combination enabled the simultaneous capture of both wide-field and super-resolution images of a sample, facilitating easier analysis and interpretation. However, this method has several limitations: (1) Precise alignment and positioning of the microsphere within the system can be complex and time-consuming, particularly for larger or intricate samples. (2) The technique's reliance on a laser source might restrict its use in certain imaging scenarios or with light-sensitive specimens. (3) The compatibility of this technique with other imaging modalities or extensions, such as multiphoton excitation or fluorescence lifetime imaging, necessitates further exploration and development.

Despite these challenges, the various implementations of static microsphere imaging have demonstrated substantial promise. Although the quality of microsphere-based images differed, the absence of previously mentioned constraints reinforces the potential for advancing microsphere-based super-resolution imaging.

IV. Microsphere-based Imaging using Dynamic Microsphere Manipulation

While static microsphere imaging offers certain benefits, the drawbacks of random microsphere placement following drop-casting frequently constrain its full capabilities. Because light propagates, only the central area of the FOV can be discerned during imaging. This region is typically around ~10 μm^2, posing challenges for accurately imaging extensive portions of a specimen. Consequently, the microsphere employed in capturing images needs to be readily maneuverable and positioned with high precision. Accurate microsphere control is often vital when examining minute specimens that surpass the diffraction limit. To overcome this hurdle, a refined technique emerged in the form of dynamic microsphere manipulation, granting substantially greater control and flexibility during imaging. This method facilitates precise microsphere manipulation and accurate positioning of the FOV, thereby augmenting the imaging potential of microspheres.

A. Imaging through Microsphere AFM Tip

Rather than creating an entirely new tool, many researchers opted to use the existing atomic force microscope (AFM) to enhance microsphere movement. Wang *et al.* introduced a technique called scanning superlens microscopy (SSUM) by merging aspects of AFM with super-resolution fluorescent microscopy.[110] A microsphere is affixed to an AFM tip for dynamic surface scanning. Images obtained during the scanning process are later digitally combined. This technique encompasses two distinct scanning approaches: non-invasive and contact modes. The former is particularly effective for sturdy samples, whereas the latter yields better results with fragile subjects. Figure 7a illustrates the setup of the apparatus. In the described setup, a microsphere is attached to an AFM cantilever, as illustrated in the images on the right side of the schematic. The choice between non-invasive or contact microscopy is determined by a mechanism that controls the interaction force.

This article has been accepted for publication in IEEE Reviews in Biomedical Engineering. This is the author's version which has not been fully edited and content may change prior to final publication. Citation information: DOI 10.1109/RBME.2024.3355875

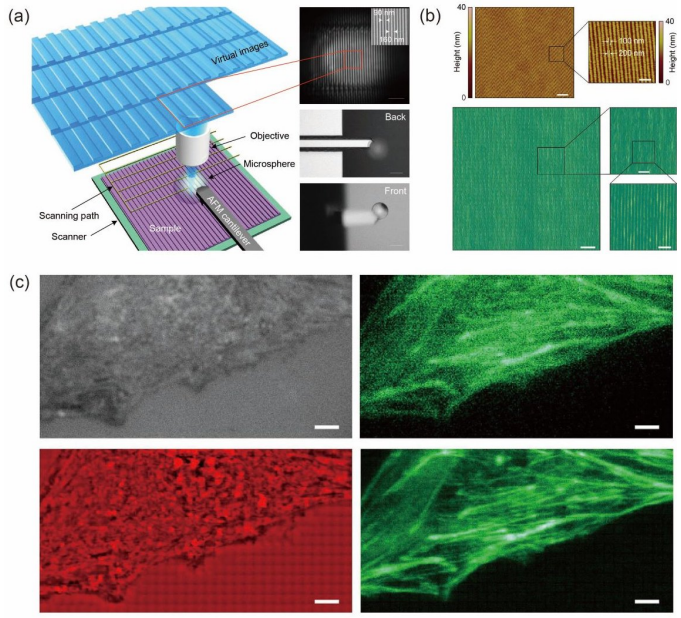

Fig. 7. Microsphere imaging with an AFM scanning system. (a) A diagram shows the setup of SSUM based on microsphere technology, integrated with an AFM scanning system. The microsphere is incorporated into the AFM cantilever to facilitate super-resolution scanning. (b) The top panel displays a Blu-ray disc's surface acquired through AFM-scan. Below, a comprehensive FOV image is digitally assembled by SSUM. (c) On the left, two panels exhibit C2C12 cell images captured using white light. The two panels on the right display fluorescence imaging of the cell. The final two images at the bottom compare AFM-scanned images with and without a 56 μm diameter microsphere. A scale bar indicating 5 μm is included for reference.[110] Copyright 2016, Nature Communications.

Furthermore, an enlarged view of a virtual image created using SSUM is depicted in Fig. 7a (top right), accompanied by an inset SEM image for comparison. Fig. 7b shows the contact scanning mode in action. The top the figure reveals a Blu-ray disc image captured through conventional AFM, whereas the lower part displays the same subject imaged via SSUM. It was observed that imaging with SSUM is significantly quicker, being about 214 times faster than standard AFM techniques. In addition, SSUM has proven effective in identifying specific structures, especially when combined with fluorescent labeling, as demonstrated in Fig. 7c.

Shortly afterward, Duocastella *et al.* conducted research regarding the capability of a microsphere affixed to an AFM cantilever through electrostatic forces.[111] The aim of this device was to offer increased accuracy by precisely maneuvering the generated photonic nanojet. Regrettably, the highest imaging resolution achieved was 260 nm, indicating that surpassing the diffraction limit remained a challenge. Nevertheless, compared to numerous existing technologies, this approach remains a cost-effective and efficient option for microscopy.

Zhang *et al.* sought to broaden the applications of AFM-based microsphere manipulation, devising a technique for nanoscale manipulation while simultaneously offering imaging at super-resolution.[112] Successful imaging of silver nanowires (80 nm in diameter) and fluorescent nanoparticles (100 nm in diameter) was achieved by attaching a $BaTiO_3$ microlens to an AFM probe. A major challenge in nanomanipulation is the difficulty in precisely observing occurrences at the nanoscale.[113] Employing microspheres for concurrent imaging and manipulation addressed this challenge, thereby enabling extremely precise nanoscale manipulation. The AFM probe was instrumental in the manipulation at the nanoscale, whereas the BaTiO3 microlens contributed to achieving high-resolution imaging.

This team subsequently devised a technology known as correlative AFM and SSUM.[114] Mirroring the earlier approach, a microlens was integrated with AFM technology for simultaneous manipulation and observation. This research, however, introduced three distinct imaging modes: rapid scanning for optical imaging using a microlens, AFM imaging for detailed surface structures, and concurrent microlens-AFM imaging. Additionally, an innovative probe, named the microlens AFM probe, was engineered to combine the microlens with AFM capabilities. The system showcased an approximately fourfold enhancement in imaging magnification and an eightfold increase in imaging speed compared to conventional AFM methods.

While previous research predominantly used an AFM for super-resolution imaging, there are other techniques for mechanical scanning that achieve similar results, like the use of a motorized stage. Huszka *et al.* developed a different approach for a microsphere-based super-resolution scanning optical microscope, aiming to improve the simplicity and accuracy of manipulating microspheres.[115] By affixing microspheres to a structure linked to a microscope's objective and methodically scanning a sample to create image segments, they could easily adjust the central FOV for capturing comprehensive, high-quality images of the entire sample. Following thorough Finite Element Method (FEM) simulations to analyze light propagation, they identified an essential separation distance of about 1 μm. Beyond this threshold, the effectiveness of super-resolution imaging diminished. Nonetheless, within this critical range, the imaged areas covered approximately 10^4 μm2, achieving resolutions ranging from 130 to 160 nm.

Addressing the same issue, Zhang *et al.* designed a device to bypass field-of-view constraints through a moving array of embedded microspheres.[116] $BaTiO_3$ microspheres were integrated into polydimethylsiloxane (PDMS) films to create arrays of microlenses. These arrays were then positioned in a 3D-printed mount, which was attached to a standard microscope, for scanning samples. In this particular study, an area of 900 μm^2 was comprehensively imaged by stitching together 210 separate scans. Moreover, the research introduced two novel imaging techniques: a dynamic-scanning imaging mode based on the microlens array and a stochastic microlens-array region imaging-overlay reconstruction mode.

Although the ability to freely adjust the microsphere and its FOV significantly improved the practicality of microsphere-based imaging, the sub-diffraction scale made dynamically observing the entire specimen a time-consuming endeavor. Furthermore, manually returning to a previous position to verify observations demanded precise movement, often proving to be cumbersome and inefficient.

This article has been accepted for publication in IEEE Reviews in Biomedical Engineering. This is the author's version which has not been fully edited and content may change prior to final publication. Citation information: DOI 10.1109/RBME.2024.3355875

Consequently, Zhou *et al.* utilized a specially designed imaging probe to capture surface images and seamlessly merge them.[117] This method eliminated the manual adjustment of the microsphere for refocusing, thus saving time compared to other dynamic techniques. The probe, as shown in Fig. 8a, comprises an array of four microspheres and a three-axis piezoelectric stage, all implemented with a conventional inverted optical microscope. The scanning process, illustrated in Fig. 8b, involves dividing the area into four sections and methodically scanning each row. The resultant images are then combined using techniques of image registration and fusion. Fig. 8c highlights the superiority of this method by contrasting it with an image acquired directly (seen on the left). Furthermore, the graph demonstrates the enhancement in sharpness and detail achieved through this scanning technique.

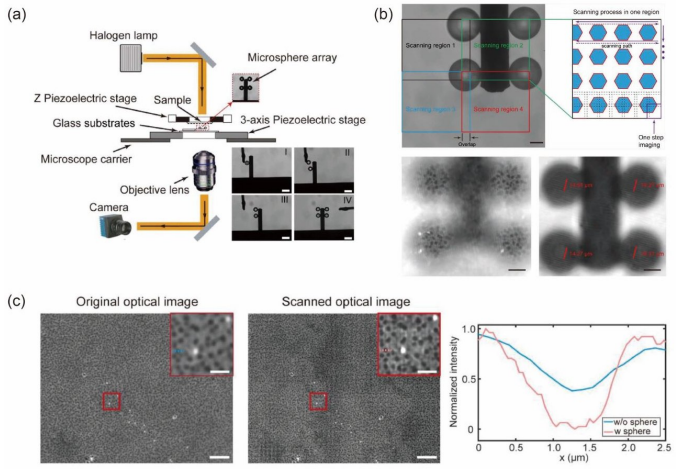

Fig. 8. Microsphere imaging with scanning using a 3-axis piezoelectric stage. (a) Illustration of a uniquely designed microsphere array integrated with a three-axis piezoelectric stage to execute scanning. (b) An explanation of the procedure is given in the top panels, followed by a demonstration of super-resolution imaging using the microsphere array. (c) A side-by-side analysis showing the differences in resolution between the initial optical image and the one obtained through scanning.[117] Copyright 2020, Journal of Optics.

It is worth mentioning that the applications of microspheres extend beyond merely visual and imaging purposes. Photonic nanojets induced by microspheres have been utilized to circumvent the diffraction limit, enabling sub-wavelength laser processing. Wen *et al.* affixed a microsphere to a movable tungsten probe, generating a nanojet that formed an optical light spot to showcase nanoscale laser patterning, thereby confirming the potential for applications beyond imaging.[118] The research also introduced a technique for real-time observation of nanoscale patterns, ensuring the integrity of tiny components throughout the process. Utilizing two distinct light paths, one dedicated to imaging and one for patterning was key to this methodology. Historically, the inability to see clearly while laser cutting components under 200 nm has prevented sub-diffraction level processing. While a 10 μm microsphere could concurrently image and process a specimen, the FOV it provided was extremely restricted, making it impractical. As a result, a 30 μm microsphere with a 5 μm FOV proved to be more suitable for this application.

The techniques discussed in this section share some common limitations that remain unaddressed. (1) Depending on the sample properties, using a microsphere may introduce unwanted optical artifacts or distortions in the resulting images. (2) Hybrid methods that combine scanning probe and optical components may be more complex and costly than certain standalone imaging techniques. (3) The approach may necessitate a longer imaging period compared to other methods, particularly when scanning extensive areas, due to the required precision in probe positioning and scanning. (4) The integration of scanning probe technology with photonic nanojets does not yield the highest possible resolution compared to more advanced nanoscale imaging techniques, such as electron microscopy.

B. Microsphere Super-Resolution Imaging Based on Optical Scanning Methods

Microsphere-based imaging offers the distinct advantage of achieving sub-diffraction resolution without necessitating a complex setup. However, the typically employed mechanical scanning method often relies on delicate and invasive AFM components, limiting its application to specialized systems. To address this issue, a non-invasive optical scanning approach has been developed to enable precise microsphere control, thereby eliminating the need for direct contact with the microspheres. Bezryadina *et al.* made one of the initial attempts to scan microspheres with optical forces by combining two pre-existing technologies: localized plasmonic structured illumination microscopy (LPSIM) and microlens microscopy, thereby creating a novel super-resolution method.[119] In their approach, polystyrene and TiO2 microspheres were captured and maneuvered on an LPSIM substrate via optical tweezers to attain the targeted resolution. The LPSIM system in this setup uses a distinct optical arrangement, commonly known as a 4f system. In this configuration, an excitation laser beam is directed through a series of components—a lens, two galvanometer scanning mirrors, and a microscope objective—before it illuminates a plasmonic substrate, triggering the required excitation. The microsphere, held in place by the optical tweezers, then functions as a microlens, facilitating the examination of the specimen enhanced by the laser, thereby achieving a resolution of approximately 75 nm.

Wen *et al.* successfully conducted microsphere-based imaging within a sealed microfluidic system, utilizing a laser-guided polystyrene microsphere lens.[120] The setup, depicted in Fig. 9a, includes a laser trapping system centered around a microsphere and a charge-coupled device (CCD) for capturing images. They employed a raster scanning pattern, as shown in Fig. 9d and Fig. 9k, and digitally assembled the individual image sections to form a comprehensive mosaic. An overview of the imaging setup is presented in Fig. 9b. Comparisons were made between a standard optical image (Fig. 9c) and the microsphere-enhanced surface images (Fig. 9e-j). The effectiveness of this method was demonstrated by imaging silver nanowires, each measuring 90 nm in diameter. Additionally, Fig. 9(l-m) demonstrate the improvement in visibility of an *E. coli* sample when a microsphere was employed. However, the integration of laser tweezers for

This article has been accepted for publication in IEEE Reviews in Biomedical Engineering. This is the author's version which has not been fully edited and content may change prior to final publication. Citation information: DOI 10.1109/RBME.2024.3355875

microsphere manipulation adds to the complexity of the setup, which may pose challenges for researchers in terms of implementation and maintenance. Moreover, the use of laser tweezers can potentially expose light-sensitive samples to the risk of photodamage due to the focused laser beam needed for microsphere manipulation.

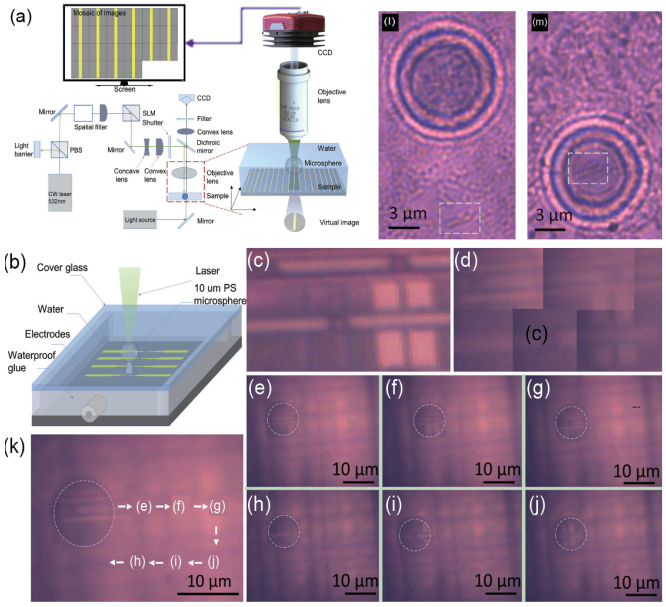

Fig. 9. Microsphere imaging *via* an optical tweezer scanning method. (a) A diagram displays the imaging mechanism that utilizes an optical tweezer for raster scanning a microsphere. In this setup, a continuous-wave laser captures a microsphere to carry out the scanning, while a CCD camera records the ensuing super-resolution images. (b) Depicts the process of imaging electrodes using the scanning microsphere. (c) Shows a reference image captured through traditional optical imaging. (d) Features a composite image created from six individual scanned images. (e-j) Represent all the microsphere positions throughout the imaging process. (k) Traces the movement trajectory of the microsphere during the imaging, propelled by the optical trapping and scanning mechanisms. (l) Imaging of *E. coli* without the aid of microspheres, resulting in diffraction-limited resolution. (m) Imaging with a microsphere, resulting in enhanced visibility of the bacterial cells.[120] Copyright 2020, Biophysical Journal.

C. Microsphere Super-Resolution Imaging via Acoustofluidic Scanning

In contrast to traditional optical tweezer-based methods, which have limitations in terms of the number of microspheres that can be controlled during scanning and necessitate modifications to the traditional optical microscope, acoustofluidic scanning methods utilize acoustofluidic forces and technology to manipulate multiple microspheres simultaneously without altering the optical microscope.[121-137] Therefore, acoustofluidic scanning methods are an appealing option for various imaging applications requiring a large FOV *via* high-precision control of multiple microspheres in a fluidic environment.

Acoustofluidic scanning offers several advantages, including versatility (*e.g.*, the ability to manipulate objects of various sizes (nm ~ mm)), programmability, biocompatibility, and contactless operation. Jin *et al.* demonstrated an acoustofluidic scanning nanoscope, as depicted in Fig. 10.[138] Periodic acoustic excitation was applied to 20 μm polystyrene microspheres for scanning, as shown in Fig. 10a. FEM simulations displaying the acoustic pressure distribution in the device and around the acoustically driven microspheres are displayed in Fig. 10b. Microsphere-magnified images were processed to generate a large FOV, as seen in Fig. 10c. A recursive crop-and-paste image processing method was employed to achieve the expansive FOV in the scanned image, as demonstrated in Fig. 10d. Multiple 10 × 10 μm scans were taken to image the word “DUKE" using this platform, as illustrated in Fig. 10e.

Jin *et al.* recently introduced an enhanced acoustofluidic scanning nanoscope using a dual-camera configuration, which reduced scanning errors in the image processing procedure, as shown in Fig. 10 (f-h).[139] In comparison to the previous method, the dual-camera approach scanned approximately 99% of the 200 μm area, a performance that was approximately six times better than the performance of acoustofluidic scanning without the dual camera. However, this technique still has drawbacks: (1) The platform necessitates sample compatibility with a microfluidic environment, which may not be suitable for many types of specimens. (2) The setup is complex for those unfamiliar with acoustic actuators or microfluidic device fabrication.

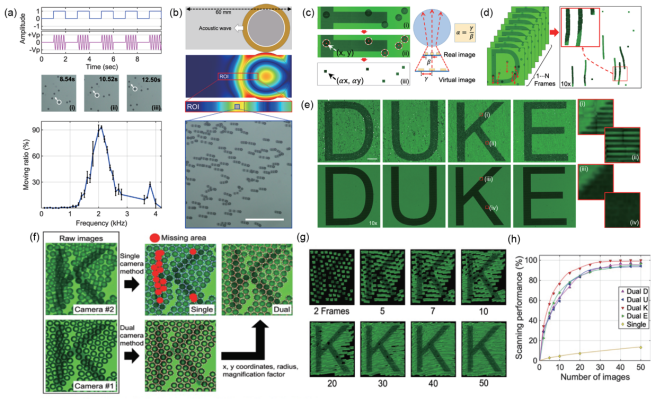

Fig. 10. Microsphere-based acoustofluidic-scanning nanoscope. (a) Acoustofluidic-based microsphere manipulation. Periodic acoustic energy was delivered to excite microspheres to push away at a 2.1 kHz operating frequency. (b) Illustration of the acoustofluidic device and the results from Finite Element Method (FEM) simulations. The composite image, with a scale bar of 300 μm, illustrates the dynamic movement of microspheres. (c) Details the image processing technique used to accomplish scanning that results in an extensive FOV. (d) Demonstrates how recursive image processing is utilized to capture the line-scanned area. (e) Presents a digitally constructed 2D image of the word 'DUKE' produced using this scanning approach. (f) Offers a comparison between systems using a single camera and those with dual cameras, highlighting the instances where the single-camera

setup fails to capture certain microsphere images, marked by red dots. (g) Shows the letter 'K' scanned with a dual-camera setup, compiling 50 images. (h) Compares the scanning efficacy of the dual-camera method against the single-camera approach.[138-139] Copyright 2020, ACS Nano. Copyright 2022, Microsystems & Nanoengineering.

V. Summary and Prospective Work

This review discussed the prominent techniques for overcoming optical diffraction limits and achieving super-resolution imaging using microspheres. We provided a concise overview of the theoretical underpinnings of photonic nanojets, the foundation for microsphere-based super-resolution imaging. We then detailed various static and dynamic microsphere imaging methods. The aspects in which each technique excelled, the drawbacks, and the resolutions achieved were identified. While static microsphere imaging attains super-resolutions, it presents challenges in controlling microsphere positions, thereby limiting the achievable FOV. Mechanical scanning techniques utilizing AFMs can easily manipulate microspheres; however, the need for AFM components meant this method would not be compatible with commercial microscopes without custom modifications. Optical scanning techniques addressed the shortcomings of mechanical scanning and used lasers to eliminate the need for a large, complex apparatus; however, there is limited depth penetration, and light-sensitive samples run the risk of photodamage. Lastly, the acoustofluidic scanning technique achieved microsphere manipulation by using acoustic forces. This scanning method, which involves recursive image cropping and pasting, enables precise control of a large array of microspheres to scan a large area resulting in an expansive digital FOV. However, the acoustofluidic scanning nanoscope involves many elements that are often difficult for biologists to implement or maintain, including acoustic streaming control, microfluidic device fabrication, and optical imaging.

While there are various established techniques for attaining super-resolution, imaging with microspheres offers practical benefits due to its efficiency. The static imaging methods described here are straightforward, economical, and don't require labeling. Scanning techniques, on the other hand, facilitate increased throughput and encompass a wider FOV. Furthermore, imaging with microspheres is versatile and can be tailored for numerous applications, such as real-time analysis in cell biology, semiconductor inspection and processing, as well as nanostructure production.

There are many aspects of microsphere-based nanoscopy that can still be improved in future studies. The imaging resolution can be significantly improved. The presence of various types of aberrations, such as spherical, chromatic, and field curvature, contributes to the decrease in resolution. By altering the size, refractive index, and shape of the microspheres used, future studies can minimize or digitally correct the effects of aberration while simultaneously determining the most effective experimental setup. Additionally, implementing achromatic lenses or different microscopes with improved microspheres could minimize these aberration losses. Successfully optimizing a configuration where aberration is negligible would propel the development of microsphere-based nanoscopy.

Another application of microsphere-based nanoscopy that has yet to be explored is its potential in 3D imaging. 3D imaging based on microspheres has not been successfully implemented due to the following challenges: (1) 3D imaging requires precise control of the relative position of an imaging microsphere to a sample surface in three dimensions. This challenge could potentially be solved by using either an AFM probe or optical tweezers or acoustic tweezers; however, this would come at the cost of significantly reduced imaging speed. (2) Even though the microsphere or sample can be controlled in 3D, its 3D position must be carefully calibrated for seamless aftermath imaging stitching. (3) Refractive index mismatch and strong spherical aberration exist for imaging in the third (z) direction, which can be potentially compensated with adaptive optics, but at the cost of significantly increased system complexity and cost. (4) High resolution requires the use of a microsphere with a higher refractive index; however, the focal position of such a microsphere is typically very close to the surface of the microsphere, which limits its maximum imaging depth and magnifies its spherical aberration. New methodologies or ideas are required to overcome these technical challenges in future studies.

As a rapidly developing area of microscopy, microsphere-based nanoscopy holds immense potential for observing and understanding nanoscale structures. With its unique advantages, such as biocompatibility and ease of use with existing imaging modalities, this technique is poised to become a powerful research tool. Combined with advances in computational image processing and the reduction in costs of digital cameras and optics, the development and implementation of novel microsphere techniques may lead to further improvements in super-resolution imaging. These advancements in making super-resolution imaging more accessible to researchers will only contribute to more discoveries across a wide range of scientific disciplines.

VI. Acknowledgment

We acknowledge support from the National Institutes of Health (R01GM143439, R01GM144417, R01GM145960, R44OD024963, and R01GM135486), National Science Foundation (CMMI-2104295), and a National Science Foundation Graduate Research Fellowship under Grant No. 2139754.

VII. Conflict of Interests:

T.J.H. has co-founded a start-up company, Ascent Bio-Nano Technologies Inc., to commercialize technologies involving acoustofluidics and acoustic tweezers. The author's (Chenglong Zhao) affiliation with the MITRE Corporation is provided for identification purposes only and is not intended to convey or imply MITRE's concurrence with, or support for, the positions, opinions, or viewpoints expressed by the author. This publication is approved for public release with case number 23-2393.

AUTHOR DETAILS

[1] Department of Biomedical Engineering, Duke University, Durham, NC 27708, USA

[2] Thomas Lord Department of Mechanical Engineering and Material Science, Duke University, Durham, NC 27708, USA

[3] Alfred E. Mann Institute, University of Southern California, Los Angeles, CA 90089, USA;

[4] The MITRE Corporation, McLean, VA 22102, USA

*TO WHOM CORRESPONDENCE SHOULD BE ADDRESSED. EMAIL: CZHAO@MITRE.ORG; TONY.HUANG@DUKE.EDU

REFERENCES

[1] Masters, B. R. History of the optical microscope in cell biology and medicine. *eLS* (2008).

[2] Araki, T. The history of optical microscope. *Mechanical Engineering Reviews* **4**, 16-00242-00216-00242 (2017).

[3] Croft, W. J. *Under the microscope: a brief history of microscopy*. **5,** (World Scientific, 2006).

[4] Heintzmann, R. & Ficz, G. Breaking the resolution limit in light microscopy. *Briefings in Functional Genomics* **5**, 289–301 (2006).

[5] Stelzer, E. H. Beyond the diffraction limit? *Nature* **417**, 806–807 (2002).

[6] Yun, S. H. *et al.* Comprehensive volumetric optical microscopy in vivo. *Nature Medicine* **12**, 1429–1433 (2006).

[7] Lichtman, J. W. & Conchello, J.-A. Fluorescence microscopy. *Nature Methods* **2**, 910–919 (2005).

[8] Taylor, D. L. & Wang, Y.-l. Fluorescence Microscopy of Living Cells in Culture, Part B: Quantitative Fluorescence Microscopy-Imaging and Spectroscopy. *Methods in Cell Biology* **30**, 1–498 (Academic Press, 1989).

[9] Betzig, E. & Trautman, J. K. Near-field optics: microscopy, spectroscopy, and surface modification beyond the diffraction limit. *Science* **257**, 189–195 (1992).

[10] Dunn, R. C. Near-field scanning optical microscopy. *Chemical Reviews* **99**, 2891–2928 (1999).

[11] Beveridge *et al.* in *Methods for General and Molecular Microbiology, Third Edition* 19–33 (American Society of Microbiology, 2007).

[12] Jonkman *et al.* Tutorial: guidance for quantitative confocal microscopy. *Nature Protocols **15***, 1585–1611 (2020).

[13] Hell, S. W. & Wichmann, J. Breaking the diffraction resolution limit by stimulated emission: stimulated-emission-depletion fluorescence microscopy. *Optics Letters* **19**, 780–782 (1994).

[14] De Lange *et al.* Cell biology beyond the diffraction limit: near-field scanning optical microscopy. *Journal of Cell Science* **114**, 4153–4160 (2001).

[15] Min *et al.* Fluorescent microscopy beyond diffraction limits using speckle illumination and joint support recovery. *Scientific Reports* **3**, 2075 (2013).

[16] Youngworth, K. S. & Brown, T. G. Focusing of high numerical aperture cylindrical-vector beams. *Optics Express* **7**, 77–87 (2000).

[17] Resolution,Nikon'sMicroscopyU,2023.https://www.microscopyu.com/microscopy-basics/resolution.

[18] J. W. Pomeroy and M. Kuball, Solid immersion lenses for enhancing the optical resolution of thermal and electroluminescence mapping of GaN-on-SiC transistors, *Journal of Applied Physics* **118**, 144501 (2015)

[19] M. Yoshita *et al.* Application of solid immersion lens to high-spatial resolution photoluminescence imaging of GaAs quantum wells at low temperatures, *Applied Physics Letters* **73**, 635–637 (1998)

[20] L. Wang *et al.* Solid immersion microscopy images cells under cryogenicconditions with 12 nm resolution, *Communications Biology* **2,** 74 (2019)

[21] Y. Zhang, C. Zheng, and Y. Zou, Focal-field distribution of the solid immersion lens system with an annular filter, *Optik* **115**, 277–280 (2004)

[22] C. D. Poweleit and J. Menéndez, Microspectroscopy Using a Solid Immersion Lens, *Microscopy and Microanalysis* **7**, 148–149 (2001)

[23] Baba *et al.* Application of Solid Immersion Lens to Submicron Resolution Imaging of Nano-Scale Quantum Wells, *Optical Review* **6**, 257–260 (1999)

[24] Mau *et al.* Fast widefield scan provides tunable and uniform illumination optimizing super-resolution microscopy on large fields. *Nature Communications* **12**, 3077 (2021).

[25] He *et al.* High-speed compressive wide-field fluorescence microscopy with an alternant deep denoisers-based image reconstruction algorithm. *Optics and Lasers in Engineering* **165**, 107541–107541 (2023).

[26] Werley, C. A., Chien, M. & Cohen, A. E. Ultrawidefield microscope for high-speed fluorescence imaging and targeted optogenetic stimulation. *Biomedical Optics Express* **8**, 5794–5813 (2017).

[27] Winter, P. W. & Shroff, H. Faster fluorescence microscopy: advances in high speed biological imaging. *Current Opinion in Chemical Biology* **20**, 46–53 (2014).

[28] Yoo, H. *et al.* Disordered nanocomposite islands for nano-speckles illumination microscopy (NanoSIM) in wide-field super-resolution imaging. *Advanced Optical Materials* **9**, 2170058 (2021)

[29] Antosiewicz, T. J. & Tomasz Szoplik. Corrugated metal–coated tapered tip for scanning near–field optical microscope. *Optics Express* **15**, 10920–10928 (2007).

[30] Doyle *et al.* Extraction of Near-Field Fluorescence from Composite Signals to Provide High Resolution Images of Glial Cells. *Biophysical Journal* **80**, 2477–2482 (2001)

[31] Seo, Y. & Wonho Jhe. High-speed near-field scanning optical microscopy with a quartz crystal resonator.

Review of Scientific Instruments **73**, 2057–2059 (2002).

[32] S. J. Bukofsky and R. D. Grober, "Video rate near-field scanning optical microscopy," *Applied Physics Letters* **71**, 2749–2751 (1997).

[33] Dickenson *et al.* Near-field scanning optical microscopy: a tool for nanometric exploration of biological membranes. *Analytical and Bioanalytical Chemistry* **396**, 31–43 (2010).

[34] Jeon *et al*. Recent advancements of metalenses for functional imaging. *Nano Convergence* **10**, 24 (2023).

[35] Pan *et al.* Dielectric metalens for miniaturized imaging systems: progress and challenges. *Light: Science and Applications* **11**, 195 (2022).

[36] Zou *et al.* Imaging based on metalenses. *PhotoniX* **1**, 2 (2020).

[37] Jeon *et al.* Recent advancements of metalenses for functional imaging. *Nano Convergence* **10**, 24 (2023).

[38] Moon *et al.* Recent Progress on Ultrathin Metalenses for Flat Optics. *iScience* **23**, 101877–101877 (2020).

[39] Lu, D. & Liu, Z. Hyperlenses and metalenses for far-field super-resolution imaging. *Nature Communications* **3**, 1205 (2012).

[40] Fang *et al.* "Sub-diffraction-limited optical imaging with a silver superlens," *Science* **308**, 534–537 (2005).

[41] Taubner *et al.* "Near-field microscopy through a SiC superlens," *Science* **313**, 1595 (2006).

[42] Liu *et al.* "Far-field optical hyperlens magnifying sub-diffraction-limited objects," *Science* **315**, 1686 (2007).

[43] X. Zhang and Z. Liu, "Superlenses to overcome the diffraction limit," *Nature Materials* **7**, 435–441 (2008).

[44] Fang *et al.* Regenerating evanescent waves from a silver superlens. *Optics Express* **11**, 682–682 (2003).

[45] Fang *et al.* Sub-Diffraction-Limited Optical Imaging with a Silver Superlens. *Science* **308**, 534–537 (2005).

[46] Lee *et al.* Optical Silver Superlens Imaging Below the Diffraction Limit. *MRS Online Proceedings Library* **919**, 401 (2006).

[47] Liu *et al.* Rapid growth of evanescent wave by a silver superlens. *Applied Physics Letters* **83**, 5184–5186 (2003).

[48] Blom H, Widengren J. Stimulated Emission Depletion Microscopy. *Chemical Reviews* **117**, 7377-7427 (2017).

[49] Vicidomini, G., Bianchini, P. & Diaspro, A. STED super-resolved microscopy. *Nature Methods* **15**, 173–182 (2018).

[50] Alonso, C. An Overview of Stimulated Emission Depletion (STED) Microscopy and Applications. *Journal of Biomolecular Techniques* **24**, S4 (2013).

[51] Bayle *et al.* Single-particle tracking photoactivated localization microscopy of membrane proteins in living plant tissues. *Nature Protocols* **16**, 1600–1628 (2021).

[52] Shroff H, White H, Betzig E. Photoactivated Localization Microscopy (PALM) of adhesion complexes. *Current Protocols in Cell Biol*ogy **41,** Chapter 41:4.21.1–4.21.27. (2013).

[53] Prabuddha Sengupta, Schuyler B. van Engelenburg, and Jennifer Lippincott-Schwartz. *Chemical Reviews* **114** , 3189–3202 (2014).

[54] Sengupta P, Lippincott-Schwartz J. Quantitative analysis of photoactivated localization microscopy (PALM) datasets using pair-correlation analysis. *Bioessays* **34**. 396–405 (2012).

[55] Rust MJ, Bates M, Zhuang X. Sub-diffraction-limit imaging by stochastic optical reconstruction microscopy (STORM). *Nature Methods* **3**. 793–795 (2006).

[56] Xu J, Ma H, Liu Y. Stochastic Optical Reconstruction Microscopy (STORM). *Current Protocols in Cytometry* **81**, 12.46.1–12.46.27 (2017).

[57] Sebastian *et al.* Direct stochastic optical reconstruction microscopy with standard fluorescent probes. *Nature Protocols* **6**, 991–1009 (2011).

[58] Pfender *et al.* Single-spin stochastic optical reconstruction microscopy. *Proceedings of the National Academy of Sciences of the United States of America* **111**, 14669–14674 (2014).

[59] Bates, M., Jones, S. A. & Zhuang, X. Stochastic Optical Reconstruction Microscopy (STORM): A Method for Superresolution Fluorescence Imaging. *CSH Protocols* **2013**, 498–520 (2013).

[60] Li, X., Wu, Y., Su, Y. et al. Three-dimensional structured illumination microscopy with enhanced axial resolution. *Nature Biotechnology* **41**, 1307–1319 (2023).

[61] Saxena, M., Gangadhar Eluru & Sai Siva Gorthi. Structured illumination microscopy. *Advances in Optics and Photonics* **7**, 241–275 (2015).

[62] Tosi *et al.* Evaluation of sensors. *Elsevier eBooks,* 283–291 (2022).

[63] Heintzmann R., Huser T. *Chemical Reviews* **117**, 13890–13908 (2017).

[64] Manton James D. 2022 Answering some questions about structured illumination microscopy *Phil. Trans. R. Soc. A.* **380**, (2021)

[65] Lee *et al.* in *Plasmonics in Biology and Medicine XIX* **11978**, 71–76 (2022).

[66] Schermelleh *et al.* Subdiffraction multicolor imaging of the nuclear periphery with 3D structured illumination microscopy. *Science* **320**, 1332–1336 (2008).

[67] Markaki *et al.* The potential of 3D-FISH and super-resolution structured illumination microscopy for studies of 3D nuclear architecture: 3D structured illumination microscopy of defined chromosomal structures visualized by 3D (immuno)-FISH opens new perspectives for studies of nuclear architecture. *Bioessays* **34**, 412–426 (2012).

[68] Markaki *et al.* Fluorescence in situ hybridization applications for super-resolution 3D structured illumination microscopy. *Methods in Molecular Biology* **950**, 43–64 (Springer, 2013).

[69] Klar *et al.* Fluorescence microscopy with diffraction resolution barrier broken by stimulated emission.

Proceedings of the National Academy of Sciences **97**, 8206–8210 (2000).

[70] Hein, B., Willig, K. I. & Hell, S. W. Stimulated emission depletion (STED) nanoscopy of a fluorescent protein-labeled organelle inside a living cell. *Proceedings of the National Academy of Sciences* **105**, 14271–14276 (2008).

[71] Huang *et al.* Three-dimensional super-resolution imaging by stochastic optical reconstruction microscopy. *Science* **319**, 810–813 (2008).

[72] Xu, J., Ma, H. & Liu, Y. Stochastic optical reconstruction microscopy (STORM). *Current protocols in cytometry* **81**, 12.46.11–12.46.27 (2017).

[73] Rust, M. J., Bates, M. & Zhuang, X. Sub-diffraction-limit imaging by stochastic optical reconstruction microscopy (STORM). *Nature methods* **3**, 793–796 (2006).

[74] Huang *et al.* Three-Dimensional Super-Resolution Imaging by Stochastic Optical Reconstruction Microscopy, *Science* **319**, 810–813 (2008).

[75] Zhong, H. Photoactivated localization microscopy (PALM): an optical technique for achieving~ 10-nm resolution. *Cold Spring Harbor protocols* **2010**, pdb. top91 (2010).

[76] Shroff, H., White, H. & Betzig, E. Photoactivated localization microscopy (PALM) of adhesion complexes. *Current protocols in cell biology* **58**, 4.21. 21–24.21. 28 (2013).

[77] Q. Wu, L. P. Ghislain, and V. B. Elings, Imaging with solid immersion lenses, spatial resolution, and applications, *Proceedings of the IEEE* **88**, 1491–1498 (2000).

[78] Serrels *et al.* Solid immersion lens applications for nanophotonic devices, *Journal of Nanophotonics* **2**, 021854 (2008).

[79] M. G. L. Gustafsson, Surpassing the lateral resolution limit by a factor of two using structured illumination microscopy, *Journal of Microscopy* **198**, 82–87 (2000).

[80] Willets *et al.* Super-resolution imaging and plasmonics, *Chemical Reviews* **117**, 7538–7582 (2017).

[81] M. Kim and J. Rho, Metamaterials and imaging, *Nano Convergence* **2**, 22 (2015).

[82] S. W. Hell and J. Wichmann, Breaking the diffraction resolution limit by stimulated emission: Stimulated-emission-depletion fluorescence microscopy, *Optics Letters* **19**, 780–782 (1994).

[83] Wang *et al.* Optical virtual imaging at 50 nm lateral resolution with a white-light nanoscope, *Nature Communications* **2**, 218 (2011).

[84] A. Darafsheh, Optical super-resolution and periodical focusing effects by dielectric microspheres, Ph.D. dissertation (University of North Carolina at Charlotte, 2013).

[85] Darafsheh *et al.* Optical superresolution by high-index liquid-immersed microspheres, *Applied Physics Letters* **101**, 141128 (2012).

[86] Darafsheh *et al.* Advantages of microsphere-assisted super-resolution imaging technique over solid immersion lens and confocal microscopies, *Applied Physics Letters* **104**, 061117 (2014).

[87] Wang *et al.* Super-resolution imaging based on cascaded microsphere compound lenses, *Applied Optics* **62**, 7868–7872 (2023)

[88] A. Darafsheh, Influence of the background medium on imaging performance of microsphere-assisted super-resolution microscopy, *Optics Letters* **42**, 735–738 (2017).

[89] Duocastella, M. *et al.* Combination of scanning probe technology with photonic nanojets. *Scientific Reports* **7**, 1–7 (2017).

[90] Ferrand, P. *et al.* Direct imaging of photonic nanojets. *Optics Express* **16**, 6930–6940 (2008).

[91] Li *et al.* Optical analysis of nanoparticles via enhanced backscattering facilitated by 3-D photonic nanojets. *Optics Express* **13**, 526–533 (2005).

[92] Lee, S., Li, L. & Wang, Z. Optical resonances in microsphere photonic nanojets. *Journal of Optics* **16**, 015704 (2013).

[93] Itagi, A. & Challener, W. Optics of photonic nanojets. *JOSA A* **22**, 2847–2858 (2005).

[94] Darafsheh, A. Photonic nanojets and their applications. *Journal of Physics: Photonics* **3**, 022001 (2021).

[95] Duan, Y., Barbastathis, G. & Zhang, B. Classical imaging theory of a microlens with super-resolution. *Optics Letters* **38**, 2988–2990 (2013).

[96] Chen, Z., Taflove, A. & Backman, V. Photonic nanojet enhancement of backscattering of light by nanoparticles: a potential novel visible-light ultramicroscopy technique. *Optics Express* **12**, 1214–1220 (2004).

[97] Devilez *et al.* Spectral analysis of three-dimensional photonic jets. *Optics Express* **16**,14200–14212 (2008)

[98] Itagi A. V. and Challener W. A. Optics of photonic nanojets *Journal of the Optical Society of America A* **22**, 2847–2858 (2005).

[99] Geints Y. E., Zemlyanov A. A., and Panina E. K. Photonic jets from resonantly excited transparent dielectric microspheres *Journal of the Optical Society of America B* **29**, 758–762 (2012).

[100] Devilez *et al.* Three-dimensional subwavelength confinement of light with dielectric microspheres *Optics Express* **17**, 2089–2094 (2009).

[101] Guo *et al.* Near-field focusing of the dielectric microsphere with wavelength scale radius *Optics Express* **21**, 2434–2443 (2013).

[102] Li, X., & Lee, K. Superresolution imaging with dielectric microspheres: Numerical investigation of the factors that influence the imaging quality. *Optics Communications* **344**, 60–69 (2015).

[103] Heifetz, A., Kong, S.-C., Sahakian, A. V., Taflove, A. & Backman, V. Photonic nanojets. *Journal of Computational and Theoretical Nanoscience* **6**, 1979–1992 (2009).

[104] Wang, Z. *et al.* Optical virtual imaging at 50 nm lateral resolution with a white-light nanoscope. *Nature Communications* **2**, 218 (2011).

[105] Li *et al.* Label-free super-resolution imaging of adenoviruses by submerged microsphere optical nanoscopy. *Light: Science & Applications* **2**, e104 (2013).

[106] Yang *et al.* Super-resolution biological microscopy using virtual imaging by a microsphere nanoscope. *Small* **10**, 1712–1718 (2014).

[107] Yang *et al.* Super-resolution imaging of a dielectric microsphere is governed by the waist of its photonic nanojet. *Nano Letters* **16**, 4862–4870 (2016).

[108] Darafsheh *et al.* Optical super-resolution imaging by high-index microspheres embedded in elastomers. *Optics Letters* **40**, 5–8 (2015).

[109] Yan, Y. *et al.* Microsphere-coupled scanning laser confocal nanoscope for sub-diffraction-limited imaging at 25 nm lateral resolution in the visible spectrum. *Acs Nano* **8**, 1809–1816 (2014).

[110] Wang, F. *et al.* Scanning superlens microscopy for non-invasive large field-of-view visible light nanoscale imaging. *Nature Communications* **7**, 1–10 (2016).

[111] Surdo, S., Duocastella, M. & Diaspro, A. Nanopatterning with photonic nanojets: Review and perspectives in biomedical research. *Micromachines* **12**, 256 (2021).

[112] Zhang, T. *et al.* Microsphere-based super-resolution imaging for visualized nanomanipulation. *ACS Applied Materials & Interfaces* **12**, 48093–48100 (2020).

[113] Wen, Y. *et al.* Photonic nanojet sub-diffraction nano-fabrication with in situ super-resolution imaging. *IEEE Transactions on Nanotechnology* **18**, 226–233 (2019).

[114] Zhang, T. *et al.* Correlative AFM and Scanning Microlens Microscopy for Time-Efficient Multiscale Imaging. *Advanced Science* **9**, 2103902 (2022).

[115] Huszka, G., Yang, H. & Gijs, M. A. Microsphere-based super-resolution scanning optical microscope. *Optics Express* **25**, 15079-15092 (2017).

[116] Zhang, T. *et al.* Fabrication of flexible microlens arrays for parallel super-resolution imaging. *Applied Surface Science* **504**, 144375 (2020).

[117] Zhou *et al.* Scanning microsphere array optical microscope for efficient and large area super-resolution imaging. *Journal of Optics* **22**, 105602 (2020).

[118] Wen, Y. et al. Photonic Nanojet Sub-Diffraction Nano-Fabrication With in situ Super-Resolution Imaging. *IEEE Transactions on Nanotechnology* **18**, 226–233 (2019).

[119] Bezryadina, A. *et al.* Localized plasmonic structured illumination microscopy with an optically trapped microlens. *Nanoscale* **9**, 14907–14912 (2017).

[120] Wen, Y. *et al.* Scanning super-resolution imaging in enclosed environment by laser tweezer controlled superlens. *Biophysical Journal* **119**, 2451–2460 (2020).

[121] Barnkob *et al.* Acoustic radiation-and streaming-induced microparticle velocities determined by microparticle image velocimetry in an ultrasound symmetry plane. *Physical Review E* **86**, 056307 (2012).

[122] Boluriaan, S. & Morris, P. J. Acoustic streaming: from Rayleigh to today. *International Journal of Aeroacoustics* **2**, 255–292 (2003).

[123] Meng, L. *et al.* Acoustic tweezers. *Journal of Physics D: Applied Physics* **52**, 273001 (2019).

[124] Baudoin, M. & Thomas, J.-L. Acoustic Tweezers for Particle and Fluid Micromanipulation. *Annual Review of Fluid Mechanics* **52**, 205–234 (2019).

[125] Ozcelik, A. *et al.* Acoustic tweezers for the life sciences. *Nature Methods* **15**, 1 (2018).

[126] Ozcelik, A. *et al.* Acoustofluidic rotational manipulation of cells and organisms using oscillating solid structures. *Small* **12**, 5120–5125 (2016).

[127] Wu, M. *et al.* Acoustofluidic separation of cells and particles. *Microsystems & Nanoengineering* **5**, 32 (2019).

[128] Rufo *et al.* Acoustofluidics for biomedical applications. *Nature Reviews Methods Primers* **2**, 1–21 (2022).

[129] Li, P. & Huang, T. J. Applications of acoustofluidics in bioanalytical chemistry. *Analytical chemistry* **91**, 757–767 (2018).

[130] Guo, F. *et al.* Controlling cell–cell interactions using surface acoustic waves. *Proceedings of the National Academy of Sciences* **112**, 43–48 (2015).

[131] Zhang, S. P. *et al.* Digital acoustofluidics enables contactless and programmable liquid handling. *Nature Communications* **9**, 2928 (2018).

[132] Tian, Z. *et al.* Dispersion tuning and route reconfiguration of acoustic waves in valley topological phononic crystals. *Nature Communications* **11**, 762 (2020).

[133] Harmonic acoustics for dynamic and selective particle manipulation, *Nature Materials* **21**, 540–546 (2022).

[134] Acoustic tweezers for high-throughput single-cell analysis. *Nature Protocols* **18**, 2441–2458 (2023).

[135] Programmable acoustic metasurfaces. *Advanced Functional Materials* **29**, 1808489 (2019).

[136] Acoustic microfluidics. *Annual Review of Analytical Chemistry* **13**, 17–43 (2020).

[137] A sound approach to advancing healthcare systems: the future of biomedical acoustics. *Nature Communications* **13**, 3459 (2022).

[138] Jin, G. *et al.* Acoustofluidic Scanning Nanoscope with High Resolution and Large Field of View. *ACS Nano* **14**, 8624–8633 (2020).

[139] Jin, G. *et al.* An acoustofluidic scanning nanoscope using enhanced image stacking and processing. *Microsystems & Nanoengineering* **8**, 1–8 (2022).

This article has been accepted for publication in IEEE Reviews in Biomedical Engineering. This is the author's version which has not been fully edited and content may change prior to final publication. Citation information: DOI 10.1109/RBME.2024.3355875